ELSEVIER

Journal of Structural Geology 30 (2008) 525–538

JOURNAL OF STRUCTURAL GEOLOGY

www.elsevier.com/locate/jsg

Clay quantification and Ar–Ar dating of synthetic and natural gouge: Application to the Miocene Sierra Mazatán detachment fault, Sonora, Mexico

Samuel H. Haines*, Ben A. van der Pluijm

Department of Geological Sciences, University of Michigan, 1100 N. University Ave, 2534 C.C. Little Bldg, Ann Arbor, MI 48109, USA

Received 7 February 2007; received in revised form 18 October 2007; accepted 28 November 2007
Available online 5 December 2007

Abstract

Direct dating of brittle fault rocks has been predicated on the assumption that illite in fault gouge is a mixture of two populations of clays: one detrital, derived from the wall rock, and the other authigenic, forming in the brittle fault zone during faulting. Owing to complex diagenetic histories of wallrock shales in previous fault-dating studies, this assumption has remained largely untested. We demonstrate the validity of our clay quantification technique using calculated WILDFIRE© patterns to accurately model both artificial mixtures of $2M_1$ and $1M_d$ illite, and natural mixtures in young fault gouges. Using our quantification approach, we obtain well-defined detrital and authigenic ages from the Sierra Mazatán metamorphic core complex in Sonora, Mexico. Because the age population of the wall rock is well constrained by cooling ages, we confirm that the detrital component in the gouge is the age of the footwall granite, while the age of the authigenic component is the time at which faulting ceased, which is in agreement with field constraints. Based on the Ar–Ar age and the thermal conditions for the growth of the authigenic illite we also conclude that the Sierra Mazatán detachment continued slipping in the brittle regime at strain rates similar to those for the plastic regime (on the order of 10^{-14} s^{-1}).

Keywords: Clay gouge; Illite polytypism; Argon–argon dating; WILDFIRE©; Sierra Mazatán

1. Introduction

In recent years, mineral reactions related to faulting in the brittle regime have been recognized as an important process in fault zones (e.g., Pevear, 1999; Vrolijk and van der Pluijm, 1999; Yan et al., 2001). In clay gouge, earlier workers isolated a fine-grained fraction of illite (<2 μm) of the 1M or $1M_d$ polytype, considered to be indicative of low-temperature authigenic growth. It was assumed that there was no detrital ($2M_1$) illite in these samples (e.g. Lyons and Snellenburg, 1970; Kralik et al., 1987). Dating of the illite tended to overestimate the age of the faulting, however, as later work has shown that some detrital material is typically present even in very fine size fractions (Pevear, 1992; Grathoff et al., 2001). Subsequent workers employed and modified modeling programs such as NEWMOD© (Reynolds and Reynolds, 1996) and WILDFIRE (Reynolds, 1993) to quantitatively determine the amounts of authigenic and detrital clays in various size fractions in a gouge (Vrolijk and van der Pluijm, 1999; Ylagan et al., 2002; Solum and van der Pluijm, 2005, 2007; van der Pluijm et al., 2006). The percentage detrital illite of each of the size fractions is plotted against their apparent Ar–Ar total gas ages, and extrapolated to 0% and 100% to find the end-member ages. Two mineralogical reactions have been used for dating fault gouge: the illitization of illite/smectite (I/S) and the neocrystallization of authigenic $1M/1M_d$ illite (shown diagrammatically in Fig. 1). Clay-rich gouges have been observed to have higher percentage of illite in illite/smectite than the wall rocks on either side (Vrolijk and van der Pluijm, 1999). Using NEWMOD©, a program that generates calculated diffraction patterns for illite and illite/smectite, workers

* Corresponding author. Tel.: +1 734 646 0512; fax: +1 734 763 4690.
E-mail address: shhaines@umich.edu (S.H. Haines).

0191-8141/$ - see front matter © 2007 Elsevier Ltd. All rights reserved.
doi:10.1016/j.jsg.2007.11.012

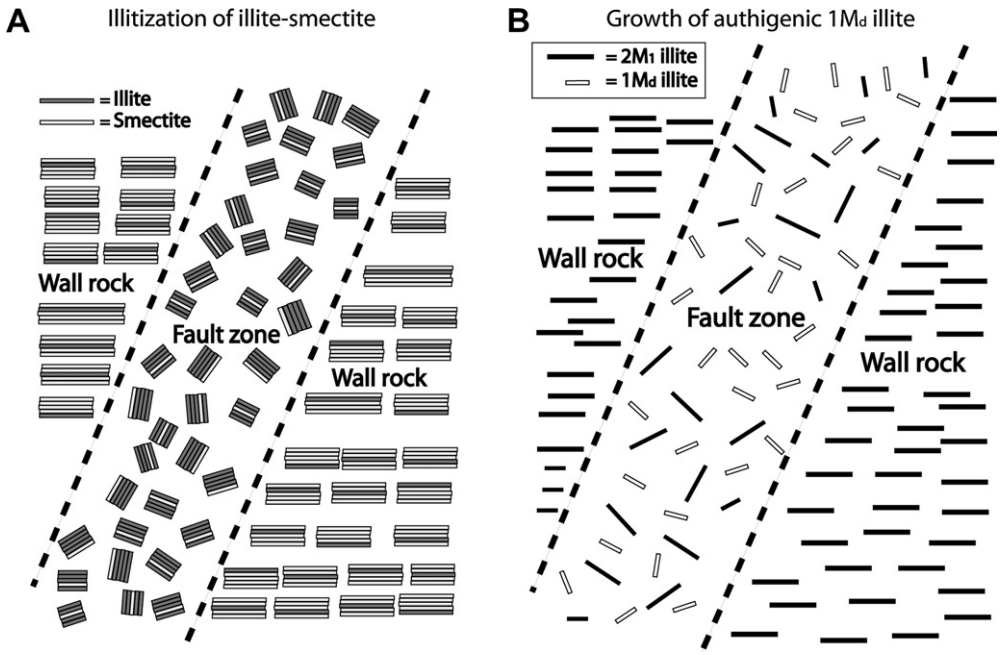

Fig. 1. Mineral transformations observed in clay gouges that are suitable for dating by illite age analysis. (A) Illitization of illite-smectite in fault gouge relative to the wall rock. (B) Growth of authigenic discrete $1M_d$ illite in the gouge. 1Md illite grows below 150 °C.

have been able to quantify authigenic illite in the illite/smectite in fault zones and reliably date the age of faulting by Ar/Ar chronology (van der Pluijm et al., 2001). The illitization of illite/smectite approach is limited when illite (assumed to be detrital, either muscovite or $2M_1$ illite) occurs both in the wall rock and grows authigenically in the fault zone as the low-temperature $1M/1M_d$ polytype (Solum and van der Pluijm, 2005). For this reason, our recent work has been focused on dating the observed $1M/1M_d$ illite, discriminating it from the detrital $2M_1$ polytype on the basis of XRD patterns and WILDFIRE©, a program that generates synthetic XRD patterns for clay minerals. WILDFIRE© patterns are used to iteratively model the percentage of the $2M_1$ and $1M_d$ polytypes in several size fractions, each with its own ratio of detrital to authigenic illite (Fig. 2) (Ylagan et al., 2002; Solum and van der Pluijm, 2005, 2007).

Our goals in this paper are threefold: to test our polytype quantification approach using experimental mixtures, to test our ability to date young gouges by applying our dating method to young, well-constrained faults, and to establish the significance of ages extracted for the detrital component of gouge. Using mixtures of standards, we aim to first demonstrate that a lowest-variance approach to modeling polytype ratios is appropriate at some ratios of polytypes, but at other ratios of polytypes, particularly $2M_1$-rich ratios, better results are obtained by matching the specific $2M_1$ peaks, rather than the entire XRD pattern. We will then demonstrate the efficacy of our technique by dating gouge from the Sierra Mazatán metamorphic core complex in northwest Mexico, where the age of the detrital component is well established by a set of cooling histories from modeled K-feldspar Ar–Ar multi-domain diffusion modeling (Wong and Gans, 2003), and show that our approach accurately captures the age of authigenic clay in fault gouge. Dating the deformation related to the onset of exhumation of a core complex in the plastic regime has become relatively straightforward (e.g. McGrew and Snee, 1994; Vanderhaeghe et al., 2003), but determining when activity on a detachment ceases, critical to understanding the kinematics of core complex evolution, is much more difficult. Activity on brittle faults at core complexes has traditionally been dated by 'bracketing', dating events that preceded and followed the faulting (e.g. Miller and John, 1999; Wong and Gans, 2003), or by inferences from thermochronometer ages (Miller et al., 1999; Carter et al., 2006). Frequently, the constraints placed on the termination of fault slip are not well defined when compared to the earlier evolution of these structures. The work presented herein provides a rigorous foundation to the Ar dating of gouge, and constrains the end of fault slip and extends the application of brittle fault dating to faults as young as mid-Miocene in age.

2. Fault dating and illite polytypism

2.1. Fault dating

Previous work dating clay gouge has encountered two common obstacles. First, while the age of the authigenic component of clay gouge extrapolated from illite age analysis could readily be related to the age of faulting, the extrapolated age of the detrital component is frequently difficult to interpret geologically, as it varies markedly from the depositional age of the hanging wall or footwall. In addition, all previous studies have focused on faults where the wall rock is sedimentary. It has long been known that illite in shale is a mixture of detrital mica, its weathering products and authigenic illite growing

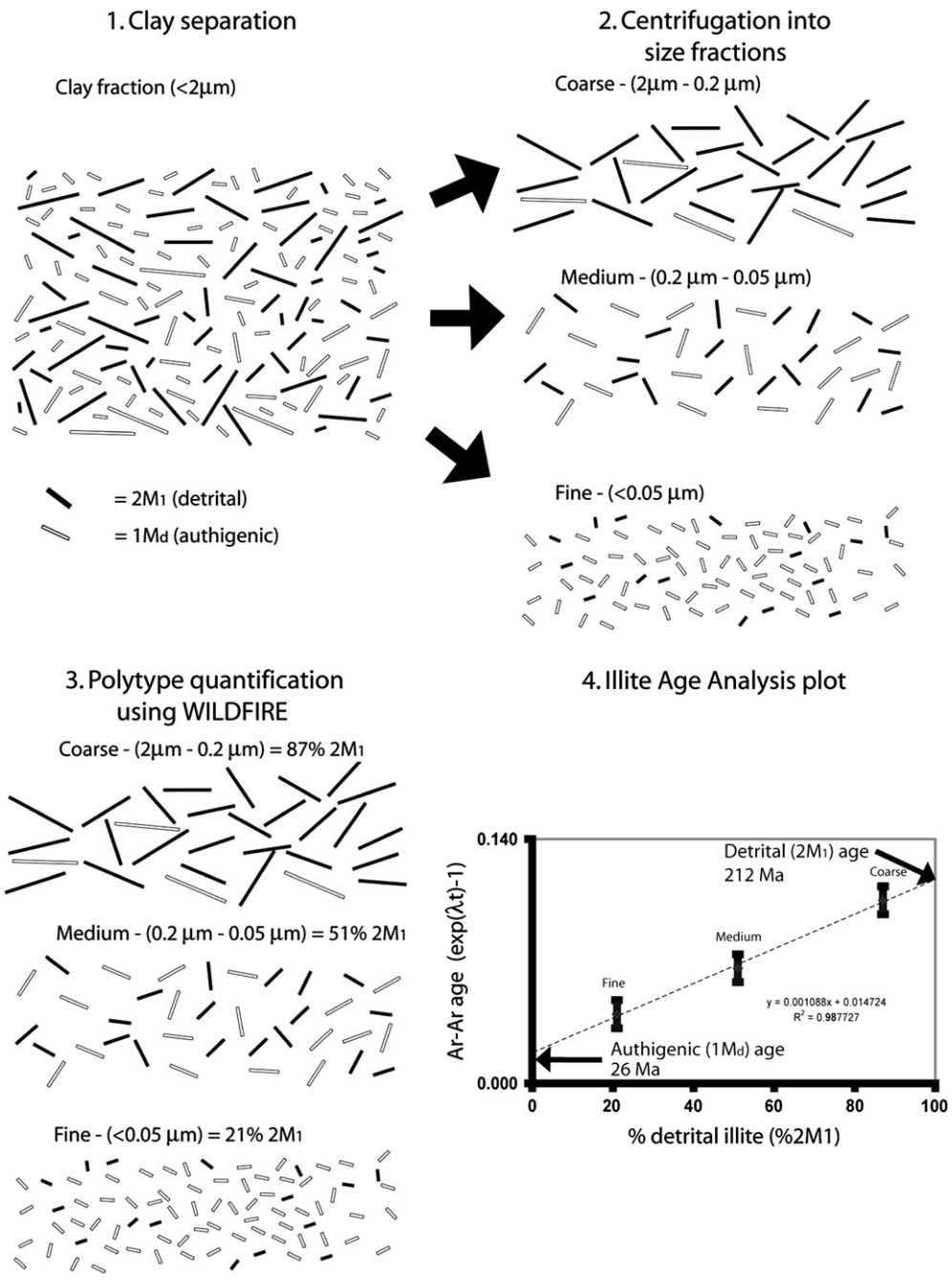

Fig. 2. Schematic figure illustrating fault gouge sample preparation and illite age analysis process. (1) The clay-sized fraction of gouge is separated by settling in water. (2) The clay-sized fraction is centrifuged into three size fractions, spanning two orders of magnitude in grain size. (3) The relative abundance of $2M_1$ and $1M_d$ illite in each size fraction is determined using WILDFIRE©. (4) The percentage of detrital illite is plotted against the Ar–Ar age. The percentage detrital illite ($2M_1$) is plotted against the function $e^{\lambda t} - 1$, where λ is the decay constant of potassium, and t is time; the percentage of detrital illite is actually linearly related to the exponential decay of potassium and not to chronological time.

during diagenesis (Bailey et al., 1962). It also has long been recognized that the K–Ar age of a shale decreases systematically with grain size (Hower et al., 1963; Velde and Hower, 1963; Clauer et al., 1997) and that the abundance of the $2M_1$ polytype relative to the $1M/1M_d$ polytype also decreases systematically with grain size (Pevear, 1992; Grathoff et al., 1998). These paired observations led to the widely accepted interpretation that the $2M_1$ component in a mixed illite population is detrital, while the $1M/1M_d$ component is authigenic (Hower et al., 1963; Reynolds, 1963; Grathoff et al., 2001).

This distinction between illite polytypes is applied to fault dating by assuming that the $2M_1$ component is detrital material derived from the wall rock, and the $1M/1M_d$ component is authigenic material formed in the fault zone during fault slip. Given the potential complexity of the mica populations

in shales, especially when both the hanging-wall and footwall are shales, the assumption that gouges are a binary mixture of detrital and authigenic illite may best be tested in an area where the age of the detrital component is well known, and the population of detrital minerals is functionally monotonic in age. A highly extended area, such as a metamorphic core complex is ideal for such an application in that the footwall rocks pass through the temperature ranges of detrital minerals for which Ar–Ar data can provide meaningful geological data (muscovite, 375 ± 25 °C, and K-feldspar 100–500 °C; McDougall and Harrison, 1999; Harrison et al., 2005) very rapidly, ensuring a nearly monotonic age population of detrital minerals.

2.2. Illite polytypism

Polytypism is a special case of polymorphism common to clay minerals and micas in that the two-dimensional arrangement of the silicate sheets remains unchanged, but the stacking sequence of the sheets varies. Traditionally, of the six possible mica polytypes (Smith and Yoder, 1956), five polytypes were identified in illite, the 1M, $1M_d$, $2M_1$, $2M_2$, and 3T polytypes (Levenson, 1955; Shimoda, 1970). The $2M_1$ polytype stacking sequence is characterized by regular 120° rotations of the 2:1 layers with a two-layer repeat, e.g. each second layer is oriented the same way. This regular stacking produces a series of distinctive (11*l*) and (02*l*) reflections at 3.72, 3.49, 3.20, 2.98, 2.86, and 2.79 Å on an X-ray powder pattern (Moore and Reynolds, 1997), shown in Fig. 3. The 1M polytype, *sensu stricto*, has an ordered monoclinic symmetry, in which all sheets are oriented the same way, while the $1M_d$ polytype stacking sequence is characterized by rotations of each silicate sheet in random multiples of 120°, or more rarely 60° relative to the sheet above and below. The 1M polytype is quite rare, and is generally only found in hydrothermal systems, where the 1M structure may be a function of anomalously high Mg contents (Peacor et al., 2002). The $1M_d$ polytype is identifiable by its lack of the $2M_1$ peaks on XRD powder patterns, and instead has broad peaks on either side of the (003) peak at 24.3° and 29.1° 2Θ (Fig. 3). The 1M and $1M_d$ polytypes are not truly distinct polytypes, but rather end-members of a spectrum of ordering of rotation of the silicate sheets (Bailey, 1988), best thought of as a single 1M-$1M_d$ polytype. The degree of ordering of the silicate sheets is expressed in percentages of zero rotation; e.g. a sheet in a perfectly ordered 1M structure will have no rotations, so the percentage zero rotations = 1.0. A perfectly disordered $1M_d$ structure will have a 1/3 chance of having a zero rotation, so the percentage of zero rotations = 0.33. For the sake of brevity and for consistency with previous work, hereafter, the subdivisions of the 1Md-1M series, the cv1M/$1M_d$ and tv1M/$1M_d$ polytypes of Drits et al. (1984) are collectively referred to as the 1M/$1M_d$ polytype unless otherwise noted.

Illite polytypism is of geological interest because it has been linked to environmental conditions of clay formation. Experimental work indicates that the $2M_1$ polytype is the most stable illite polytype and is thought to form above 280 °C (Yoder and Eugster, 1955; Velde, 1965; Srodon and Eberl, 1984), while the 1M/$1M_d$ polytypes are thought to form at significantly lower temperatures, below approximately 200 °C (Velde, 1965). The sequence $1M_d$-1M-$2M_1$ has been proposed to be indicative of increasing temperature and pressure, with the presence of authigenic $2M_1$ indicating the onset of the lowest-temperature metamorphic zone (the anchizone 280–360°C) (Reynolds, 1963; Weaver and Brockstra, 1984). Apparently cogenetic $1M_d$, 1M and $2M_1$ are known, however, from hydrothermal systems active at 270–330 °C (Lonker and

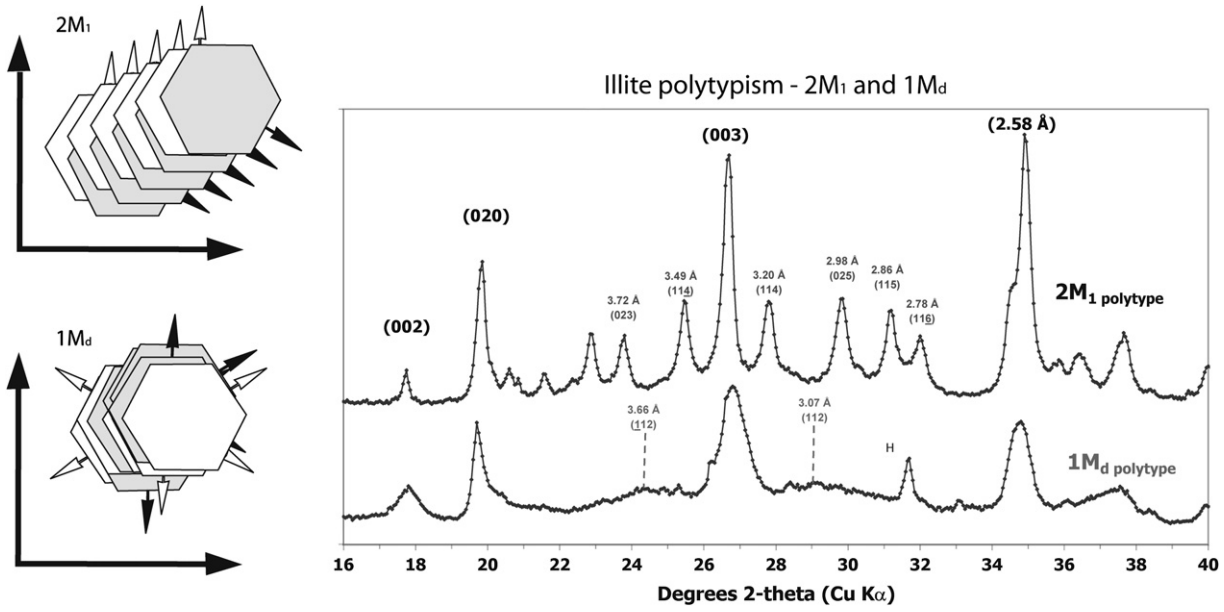

Fig. 3. Stacked XRD tracings for $2M_1$ muscovite (Owl Creek pegmatite, Wind River Mts, WY, USA) and $1M_d$ illite (IMt-1, Silver Hill, MT, USA). Note the $2M_1$-specific (11*l*) and (02*l*) peaks between 23 and 32° 2Θ produced by the $2M_1$ ordered lattice layer stacking, and the $1M_d$-specific broad (1̲12) and (112) peaks at 24.3 and 29.1° 2Θ. (H) is halite. Polytype cartoons redrawn after Moore and Reynolds (1997).

Fitz Gerald, 1990). While the upper limit on the conditions for growth of $1M/1M_d$ is thus somewhat variable, the $1M/1M_d$ polytypes are the only polytype observed in very low-grade sediments that lack a detrital illite or mica component, such as pore-filling 'hairy' illites in clean sandstones and illitized bentonites (Pevear, 1999). Work in sedimentary basins has found that the illite in sedimentary basins is nearly always a mixture of the $2M_1$ and $1M/1M_d$ polytypes (Grathoff et al., 2001). The $2M_1$ polytype is typically thought to be detrital material, while the $1M/1M_d$ illite is formed during diagenesis, as the latter are the only polytypes observed to form at temperatures below 200 °C (Grathoff et al., 2001). This observation is of key importance in considering the observed presence of $1M/1M_d$ illite in fault gouge. It is clear that the authigenic growth of $1M/1M_d$ must be occurring well below 280 °C., which is in the brittle deformation realm.

3. Geologic setting

To apply the clay quantification method to natural fault gouge and to test our ability to date faults as young as Miocene in age, we studied gouge from the Sierra Mazatán metamorphic core complex in Sonora, Mexico. Sierra Mazatán is the southernmost Cordilleran metamorphic core complex, one of a discontinuous band of highly extended domains from British Columbia to northwestern Mexico (Anderson et al., 1980; Nourse et al., 1994; Gans, 1997; Fig. 4). The complex has a 'typical' metamorphic core complex geometry, with a topographically high shield-like lower plate of mid-crustal Paleocene (58 ± 3 Ma U–Pb age, Anderson et al., 1980) granites and minor gneisses, separated from Cretaceous metavolcanics and unmetamorphosed Tertiary sedimentary strata by a shallowly west-dipping complex fault zone with a plastic-to-brittle deformation history (Vega Granillo and Calmus, 2003; Wong and Gans, 2003, 2005). The onset of exhumation at Sierra Mazatán is well constrained by K-feldspar $^{40}Ar/^{39}Ar$ ages, which indicate rapid west-directed exhumation, beginning at 20 Ma in the east, and at 18 Ma in the west. The end of exhumation is only constrained by a 12.4 Ma ignimbrite outcropping on the mylonitic carapace, indicating the mylonites were at the surface by that time (Vega Granillo and Calmus, 2003; Wong and Gans, 2003). The detachment fault is exposed on the northwest side of the core complex at the base of Cerro Pelon (UTM 0574600 E, 3226750 N, NAD 1927 Mexico UTM datum), about 10 km north along strike from the sample locations described in Wong and Gans (2003). The gouge zone is 0.5–2 m thick, and separates Cretaceous metavolcanics from weakly mylonitized and extensively fractured Paleocene granite. The gouge is a yellowish-brown hard clayey gouge with a crude visible fabric, and contains rounded and abraded clasts of granite and grains of quartz and feldspar in a matrix of very fine clay. Two K-feldspar Ar–Ar ages from footwall constrain the cooling history of the footwall in the vicinity of the detachment fault. The M1 sample of Wong and Gans (2003) is taken

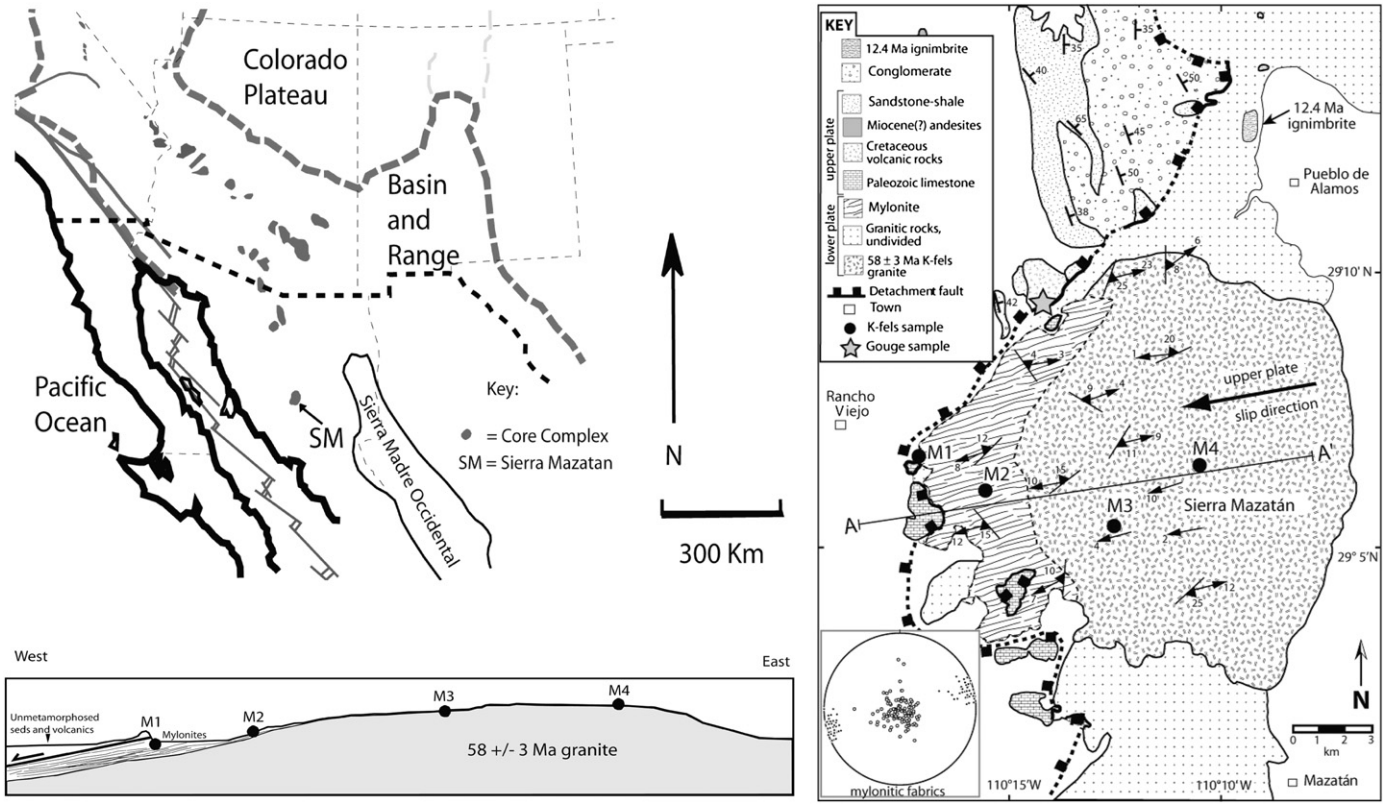

Fig. 4. Location map of northwest Mexico and surrounding areas showing location of study area and selected geographic and tectonic features. Boundaries of the Basin and Range (hachured line) and relatively un-extended Sierra Madre Occidental are modified from Coney, (1980), Gans (1997) and Wong and Gans (2003). Solid lines are faults. Geologic map and section of Sierra Mazatán from Wong and Gans (2003), courtesy of Martin Wong.

from the immediate vicinity of the fault, and records rapid cooling of the footwall of the detachment from 350 °C at 18 Ma to 200 °C at 16 Ma. The M2 locality, ~3 km up-dip from the M1 locality, and ~500 m below the detachment surface in true section, records rapid cooling from 350 °C at 19.5 Ma to 200 °C at 17.5 Ma. Both the published Ar–Ar ages, and paleomagnetic constraints on a set of post-mylonitization basaltic dikes (Wong, personal communication) clearly indicate that the fault was initiated at a dip of ~60°, and was then passively rotated in a domino fashion to its current dip of 10–20°. Dating the deformation related to the onset of exhumation of a core complex in the plastic regime has become relatively straightforward (e.g. McGrew and Snee, 1994; Vanderhaeghe et al., 2003; Wong and Gans, 2003), but determining when activity on a detachment ceases, critical in understanding the kinematics of core complex evolution, is much more difficult. Activity on brittle faults at core complexes has traditionally been dated by 'bracketing', dating events that preceded and followed the faulting (e.g. Miller and John, 1999; Wong and Gans, 2003), or by inferences from thermochronometer ages (Miller et al., 1999; Carter et al., 2006). Frequently, the constraints placed on the termination of fault slip are not well defined when compared to the earlier evolution of these structures. Key questions therefore remain, how long the core complex was active, both in the plastic and brittle regimes, and when various parts of a detachment were active.

4. Methods

4.1. Standard sample preparation

Because most commercial illite standards are taken from sedimentary basins, where illites are nearly always a mixture of polytypes (Grathoff et al., 1998), we used muscovite as a proxy for $2M_1$ illite. Muscovite has the same crystallographic structure as $2M_1$ illite and is chemically very similar. Muscovite has only slightly less Si, Mg and H_2O than illite and only slightly more tetrahedral Al and 1.0 interlayer K^+ per $(Si,Al)_4O_{10}(OH_2)$ formula unit, where illite has 0.89 K^+ per formula unit (Srodon et al., 1992). Muscovite collected from the Owl Creek pegmatite, Wind River Range, WY, was ground in a shatter box for 1 min, and then suspended in water. The clay component of the ground muscovite (<2 μm spherical equivalent) was separated using Stokes' Law for the settling of particles in water. For the $1M_d$ standard we used the IMt-1 standard from Silver Hill, MT, available from the Clay Minerals Society Source Clay Repository and characterized by Hower and Mowatt (1966). The IMt-1 illite was disaggregated in water, suspended and the clay fraction poured off in the same manner as the muscovite. The clay fraction was centrifuged to <1 μm in size, and dried by evaporation. Prior to detailed quantification, both the IMt-1 and muscovite were analyzed for the presence of non-clay phases and interlayered smectite using oriented smear preparations on a glass slide. Both standards were then X-rayed twice, once air-dried and again after solvation for 72 h in ethylene glycol from 2 to 35° 2Θ at 1 degree min^{-1} using a Scintag X1 Θ–Θ powder diffractometer, with an accelerating voltage of 40.0 kV, a filament current of 35.0 mA, and a Cu Kα source. XRD analysis indicates that both the Owl Creek muscovite and the <1 μm fraction of the IMt-1 standard are nearly monomineralic muscovite and illite, respectively. Some halite was noted in the IMt-1 material, probably derived from laboratory water used in centrifugation. Neither the peaks for the $2M_1$ sample nor for the IMt-1 sample shifted upon glycol solvation, but the IMt-1 sample had some broadening of the (001) reflection and a sloping shoulder on the low-angle side of the peak upon solvation, indicating that some smectite interlayers were present. The percentage of interlayered smectite was checked using the Δ2Θ method of Sroden (1980) and was found to be <5%. The $2M_1$ muscovite and the 1Md illite were then mixed in 6 different weight-percentage mixtures, 0% $2M_1$, 14% $2M_1$, 23% $2M_1$, 50% $2M_1$, 77% $2M_1$ and pure $2M_1$ (Fig. 5). Samples were side-loaded into an Al sample holder to achieve a high degree of particle randomness in the sample (Moore and Reynolds, 1997). Each mixture was then scanned from 16 to 44° 2Θ. Because of the low intensity of the polytype-specific peaks and the resolution of XRD increases with longer counting time at each step, we used the step-scanning mode with a step size of 0.05° and a count time of 40 s per step. Several XRD analyses of the same mixture were performed to assure that the samples were thoroughly mixed.

4.2. Sierra Mazatán sample preparation

About 0.5 kg of clay gouge material from the Sierra Mazatán detachment fault was disaggregated by soaking in water and suspended repeatedly until the sample was free of salts. The clay-sized material was separated using the same Stoke's law techniques as for the gouge sample. The accumulated clay fraction was centrifuged into a total of five different size fractions (2–1 μm, 1–0.5 μm, 0.5–0.1 μm, 0.1–0.05 μm and <0.05 μm) spanning roughly two orders of magnitude in grain size, to obtain multiple samples, each with a distinct ratio of relatively coarse-grained detrital and fine-grained authigenic illite. As the effects of chemical treatments to remove carbonate, quartz, or organic material on the retention of Ar by illite are not known (Moore and Reynolds, 1997), we did not treat our samples.

4.2.1. WILDFIRE modeling

Several methods have been used to quantify the amount of $2M_1$ and $1M/1M_d$ in illite mixtures using properties of the polytype-specific peaks. Early approaches were empirical, using standards mixed in various ratios and ratioing the area of one or two polytype-specific peaks to the area of the 2.58 Å peak at 36° 2Θ (see summary in Dalla Torre et al., 1994). A significant improvement was proposed by Grathoff and Moore (1996) who used a combination of physical mixtures and WILDFIRE© calculated XRD patterns to ratio the area of five polytype-specific peaks to the area of the 2.58 Å peak. WILDFIRE© calculates three-dimensional X-ray diffraction patterns for randomly oriented grains and allows the user to experiment with many mineralogic variables to fully capture the variability of structure ordering in illites described

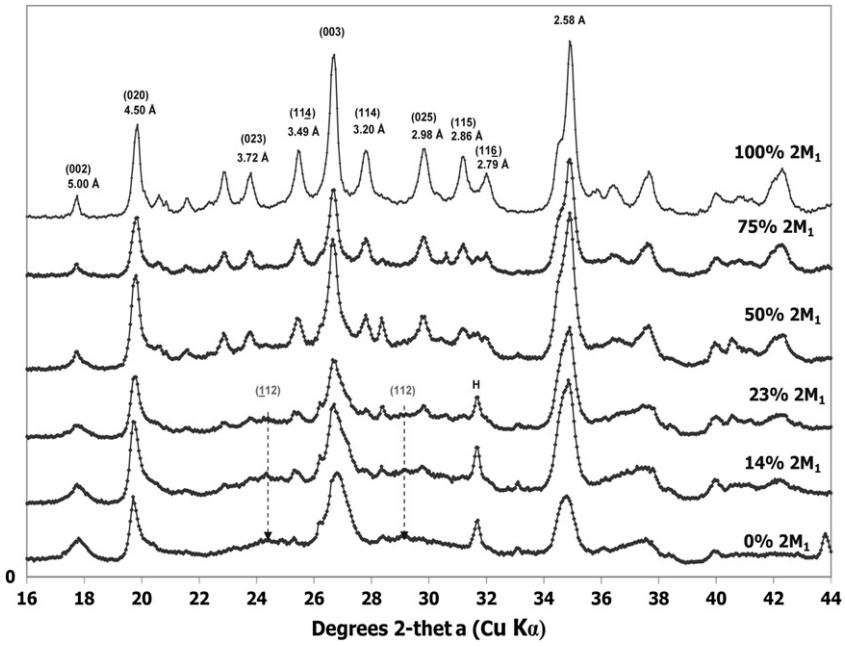

Fig. 5. Stacked XRD tracings for six artificial mixtures of Owl Creek muscovite ($2M_1$) and IMt-1 illite ($1M_d$). Note the gradual decrease in intensity of the $2M_1$-specific peaks with decreasing abundance of $2M_1$ in the mixture.

earlier. WILDFIRE© also allows the user to vary the thickness of the diffracting crystallites, the randomness of the sample (also known as the Dollase factor), the percentage of interlayered smectite, its hydration state, and any ordering of the illite/smectite (Reichweite). This multitude of options potentially allows for better matching of real powder patterns than empirical ratios of peak areas derived from a single set of standards. More recently, workers have exclusively used mixtures of WILDFIRE©-generated patterns to quantify the proportions of polytypes in a sample (Ylagan et al., 2002; Solum and van der Pluijm, 2005, 2007). This WILDFIRE©-based approach uses a least-squares lowest-variance approach to determine the best match between the sample and calculated patterns. Although the absolute number of counts recorded by an XRD unit for a given diffraction angle and sample are largely a function of machine settings and sample preparation, and are not in themselves geologically meaningful (the relative numbers of counts at different diffraction angles are however extremely meaningful), the absolute number of counts for a given diffraction angle calculated in WILDFIRE are usually much lower than the number of counts recorded by an XRD, so a scale factor must be used to multiply each WILDFIRE 'count' so that it is similar to those recorded by the XRD for the natural samples. Scale factors appropriate for our apparatus typically range from 5.0 to 30.0 and are used in increments of 0.1 At each step (0.05°) in the XRD scan of the sample pattern between 21 and 36° 2Θ, the region with the $2M_1$ polytype-specific peaks, a variance is calculated between the sample and the scaled mixture of WILDFIRE patterns in a spreadsheet. The square of the variance at each step is calculated, the squares of the variances are then summed, giving a total 'variance' for the mixture of theoretical patterns. Our approach was first to apply the lowest variance approach to the mixtures, as a test of this approach, and then to modify it where appropriate. We observe that the absolute magnitude of the scale factor rarely affects which mixture of $2M_1$ and $1M_d$ patterns has the lowest variance with the natural sample. We do however, compare results with many scale factors and for the lowest-variance approach we use the scale factor which produces the lowest absolute variance. Until now, this approach of using WILDFIRE©-generated patterns has not been tested against standards to demonstrate its validity.

4.3. Argon dating

As the momentum transfer that occurs during the $^{39}K(n,p)-^{39}Ar$ reaction is sufficient to move the produced Ar atom ~0.1 μm, (a significant percentage of the effective diameter of most clay crystallites), large amounts of ^{39}Ar might be lost during irradiation, producing erroneously old ages. To avoid this problem, the Sierra Mazatán samples were packaged into fused silica vials and sealed prior to irradiation (van der Pluijm et al., 2001). Thus, the ^{39}Ar expelled from the crystallites during irradiation is retained for analysis (see Dong et al., 1995 for a rigorous treatment of the issue). The sample vials were broken open; the initial gas was analyzed; the vials were then step-heated under a defocused laser until sample fusion occurred. The total gas age obtained from the vacuum-encapsulated sample is equivalent to that obtained from a conventional K–Ar age (Dong et al., 1995, 1997).

5. Results and quantification

The XRD peaks of interest for polytype determination are non-(00*l*) peaks and are only visible on powder patterns taken from samples with a near-random orientation of the crystallites.

For all mixtures of standards, the (020) peak at 4.5 Å (19.8° 2Θ Cu Kα) is significantly higher than the (002) peak at 5.0 Å (17.8° 2Θ), indicating that acceptable sample randomness was achieved (Grathoff and Moore, 1996). The intensity of the $2M_1$-specific peaks decreases consistently with decreasing $2M_1$ content of the mixtures (Fig. 5). We applied the lowest variance modeling approach to all 6 mixtures, and then applied our approach, which fits the entire profile from 21 to 36° 2Θ when the $2M_1$ peaks are weak or absent, but fits only the $2M_1$ peaks when they are strong. Fig. 6 shows the best matches using the lowest-variance method, while Fig. 7 shows the best matches using our method. For the $1M_d$-rich mixtures the lowest variance approach generates very good fits; the figures for the 23% $2M_1$, 14% $2M_1$ and 0%$2M_1$ mixtures needed only very minor iterative adjustment to produce visually satisfying matches. However, at high percentages of 2M1 (50% $2M_1$, 75% $2M_1$ and 100% $2M_1$), a lowest variance approach significantly underestimates the actually percentage of $2M_1$ in the mixture. The reason for this is clear in Fig. 8 which shows best matches calculated using the two different approaches. The effect of background broadening on the real XRD pattern is immediately apparent. WILDFIRE© patterns do not calculate a background level of scatter that replicates the peak broadening from amorphous phases, such as oxides and oxy-hydroxides, inevitably found in nature. The effect of the background produced by these phases is to generate

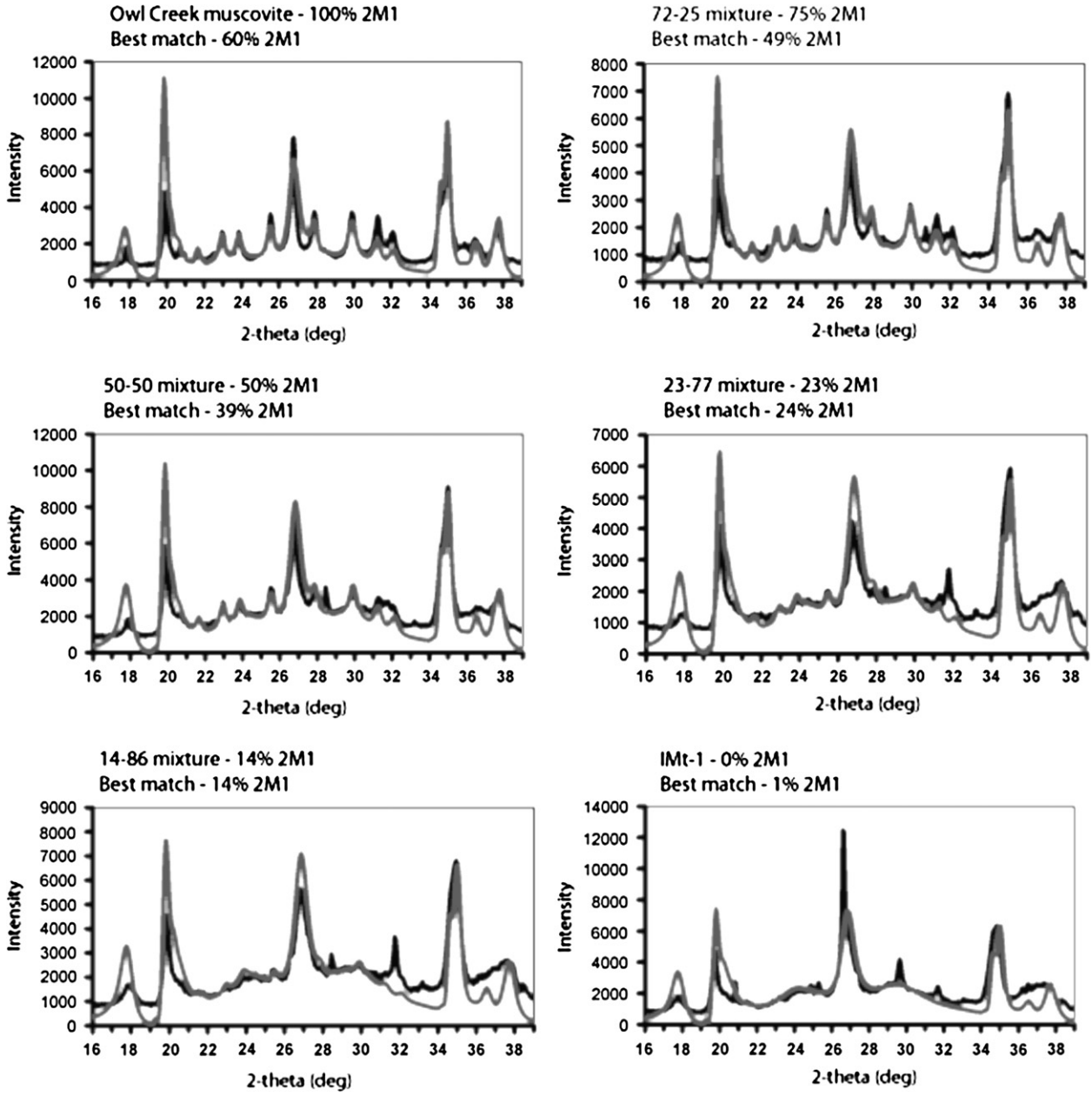

Fig. 6. Best matches of WILDFIRE patterns using WILDFIRE and a lowest-variance approach. Note the excellent visual correspondence, but that the percentage of $2M_1$ in $2M_1$-rich mixtures is severely underestimated.

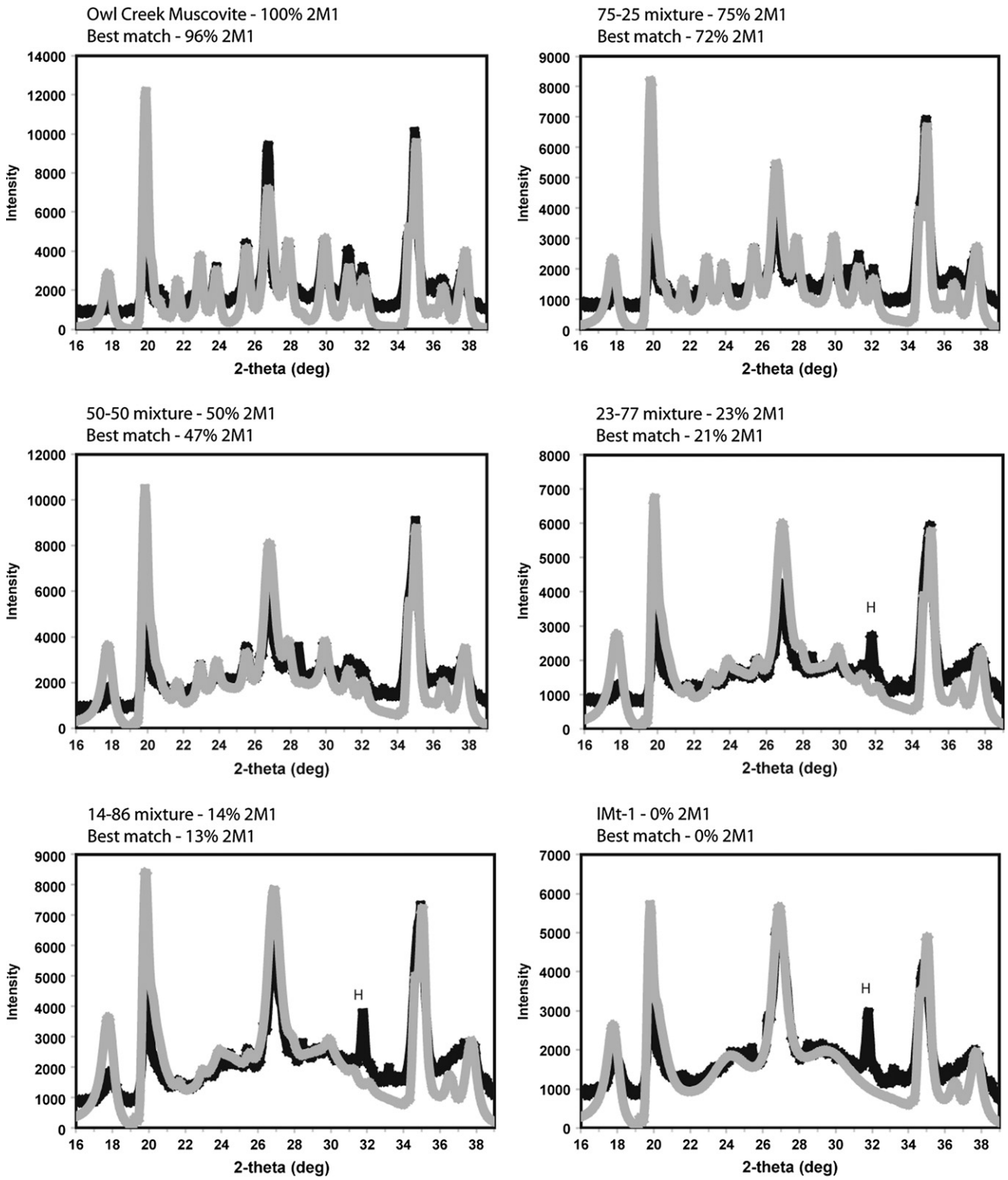

Fig. 7. XRD tracings for six artificial mixtures of Owl Creek muscovite ($2M_1$) and IMt-1 illite ($1M_d$) and best matches calculated using WILDFIRE and our approach. Note that especially for the $2M_1$-rich mixtures, the best match matches the $2M_1$-specific peaks, while for $1M_d$-rich mixtures, the best match matches the entire pattern between 21 and 36° 2Θ. H is hematite.

anomalously $1M_d$-rich matches for $2M_1$-rich mixtures, shown in Fig. 9. Of the many variables involved in matching calculated patterns to real mixtures using our approach, the relative amounts of the two end-members, the crystallite size of the calculated end-members and the Dollase factor are the most important. The results of our experiments show excellent correspondence between prepared and calculated mixtures, demonstrating the validity of our method.

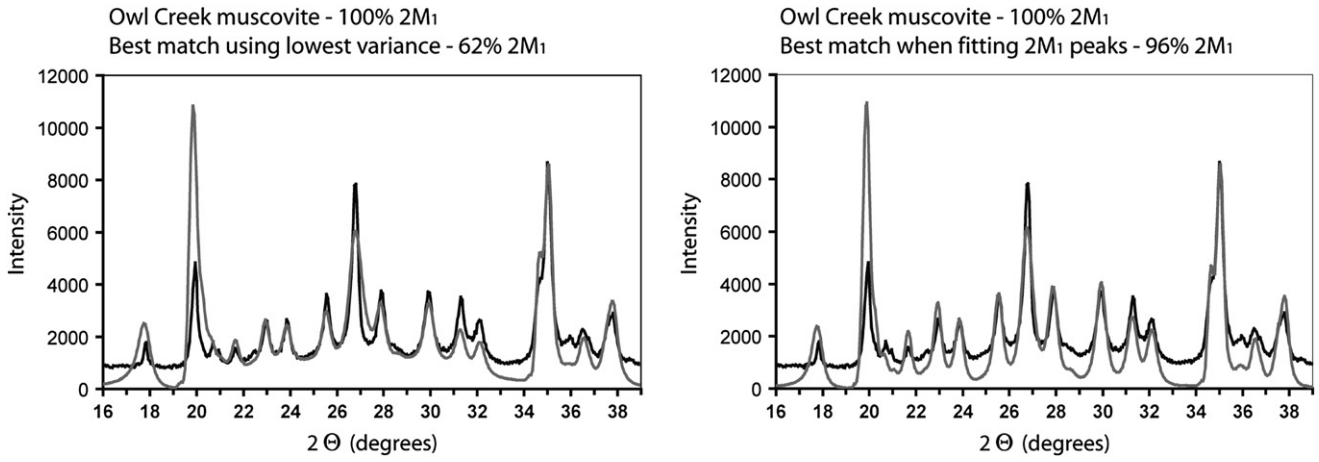

Fig. 8. Best matches of WILDFIRE patterns to XRD tracings of Owl Creek muscovite ($2M_1$, black) calculated using WILDFIRE (grey) using two different approaches. The figure on the left is calculated using a strict lowest-variance approach, while the right-hand figure is calculated using our approach. Note that the lowest-variance approach does not take into account the background broadening from the real XRD pattern between the $2M_1$-specific peaks.

Each size fraction of the sample from Sierra Mazatán was then X-rayed in the same manner as the standards and modeled using our approach; matches for the Sierra Mazatán size fractions are shown in Fig. 10. The very coarse and coarse size fractions contain an assemblage of quartz + dolomite + $2M_1$ illite + $1M_d$ illite. The medium, fine and very fine fractions have an assemblage of $2M_1$ illite or muscovite and $1M_d$ illite in varying percentages. The relative abundance of quartz and dolomite both decrease systematically with grain size of the size fraction. Significantly, none of the size fractions contains any detectable feldspar; feldspar peaks can overlap the polytype-specific peaks used for modeling, and in addition, most feldspar contains K^+, greatly complicating any attempt to date feldspar-clay mixtures using Ar–Ar methods. The modeling of the sample powder patterns indicates the samples have widely varying ratios of $1M_d$ and $2M_1$, with the percentage of $2M_1$ decreasing with decreasing grain size. The very coarse and coarse fractions contained 60% and 84% $2M_1$ respectively. The finest fraction contains only 18% $2M_1$ and consists primarily of a disordered *tv*1Md illite (percent zero rotations = 0.4, much closer to *tv*1Md than *tv*1M) with very few smectite interlayers (<10%).

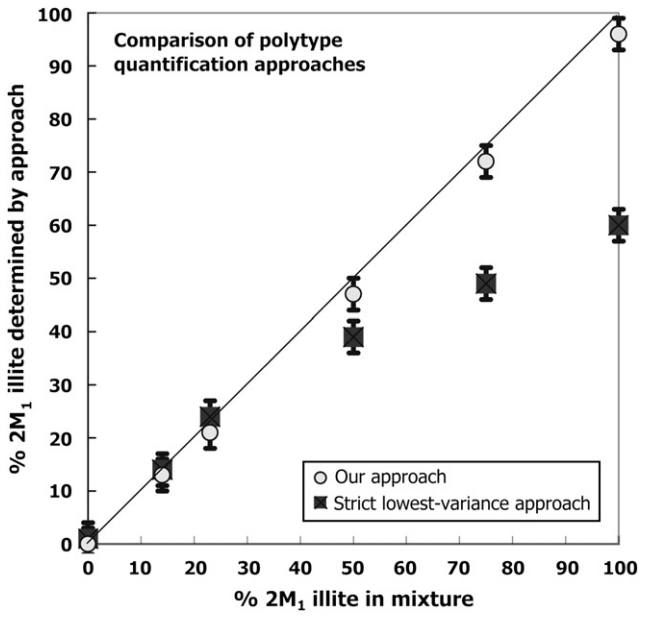

Fig. 9. Predicted vs. actual comparison of polytype quantification using a strict lowest-variance approach and our approach which uses the entire pattern between 21° and 36° 2Θ for $1M_d$-rich mixtures, while for the $2M_1$-rich mixtures, our approach focuses on matching the $2M_1$-specific peaks. Our approach is similar to the lowest-variance approach in identifying small quantities of $2M_1$ well, but is much better at identifying 2M1-rich mixtures than a strict lowest-variance approach. Error bars are ±3%.

The Ar–Ar data from the Sierra Mazatán samples are shown in Fig. 11. The Ar-release spectra for each size fraction do not have plateaus due to the effects of Ar recoil (Dong, 1995), and because they are composed of mixtures of grains of different ages and grain sizes. All the spectra have an initial near-zero-age component, interpreted to be ^{39}Ar released during irradiation due to recoil. The percentage of Ar released during the initial 'recoil' fraction increases with progressively finer size fractions, consistent with finer-grained clays having a higher surface-to-volume area and thus potential for ^{39}Ar loss during irradiation. 'Spikes' in the spectra are heating steps in which relatively little argon was released and thus have large analytical uncertainties. The very coarse size fraction released comparatively little argon and thus has large analytical errors relative to the other size fractions. XRD analysis indicated that the very coarse size fraction was composed primarily of quartz and dolomite, with relatively little illite. The coarse size fraction spectrum contains a 19.9 ± 0.3 Ma plateau-like component interpreted to be the cooling age of the $2M_1$ material in that sample vial, and is similar to the 18–20 Ma cooling ages interpolated from the same temperature ranges of the K-feldspar data of Wong and Gans (2003), taken from the vicinity of the detachment.

As our polytype modeling indicates a change in the predominant illite polytype from $2M_1$ in the coarser size fractions

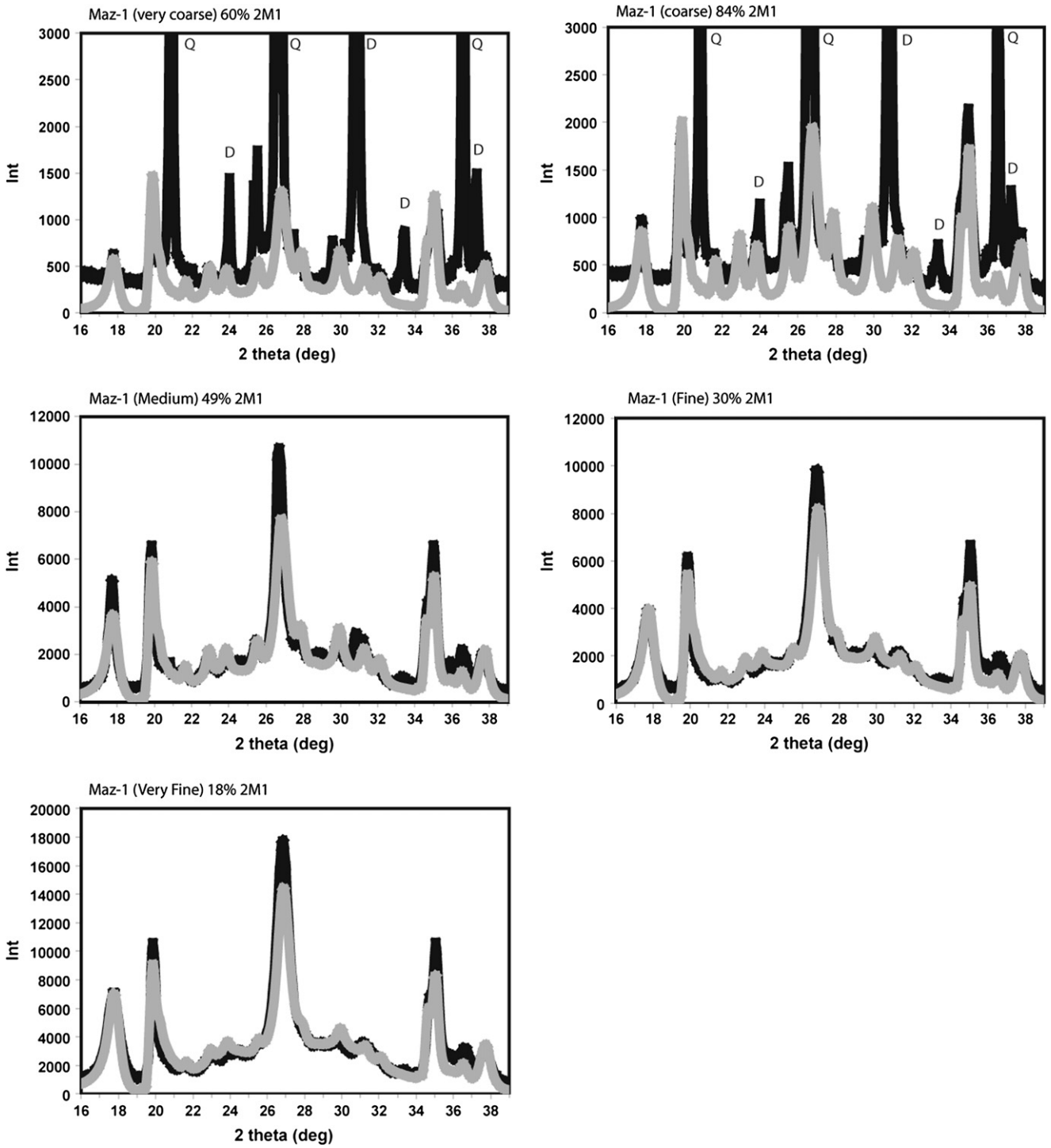

Fig. 10. XRD patterns (black) and best matches (grey) for size fractions of gouge from Sierra Mazatan. The prominent peaks extending off the graph for the very coarse and coarse fractions are peaks from non-clay phases (Q, quartz; D, dolomite).

to $1M_d$ in the finer fractions, and the Ar–Ar ages decrease as the percentage of $2M_1$ increases, it is apparent that the size fractions contain varying components of two illite populations, an older $2M_1$ polytype (probably detrital muscovite from the footwall granite) and a younger $1M_d$ formed during brittle faulting. Such transitions have been noted in brittle faults elsewhere (van der Pluijm et al., 2001; Ylagan et al., 2002; Solum and van der Pluijm, 2005, 2007) and have been dated by illite age analysis, which correlates the percentage of the $2M_1$ polytype and apparent argon age of each size and extrapolates the ages of the $1M_d$ and $2M_1$ (authigenic and detrital components). The illite age analysis plot plots the percentage detrital component against the function $e^{\lambda t} - 1$, where λ is the decay constant of argon and t is apparent age, as it is the decay

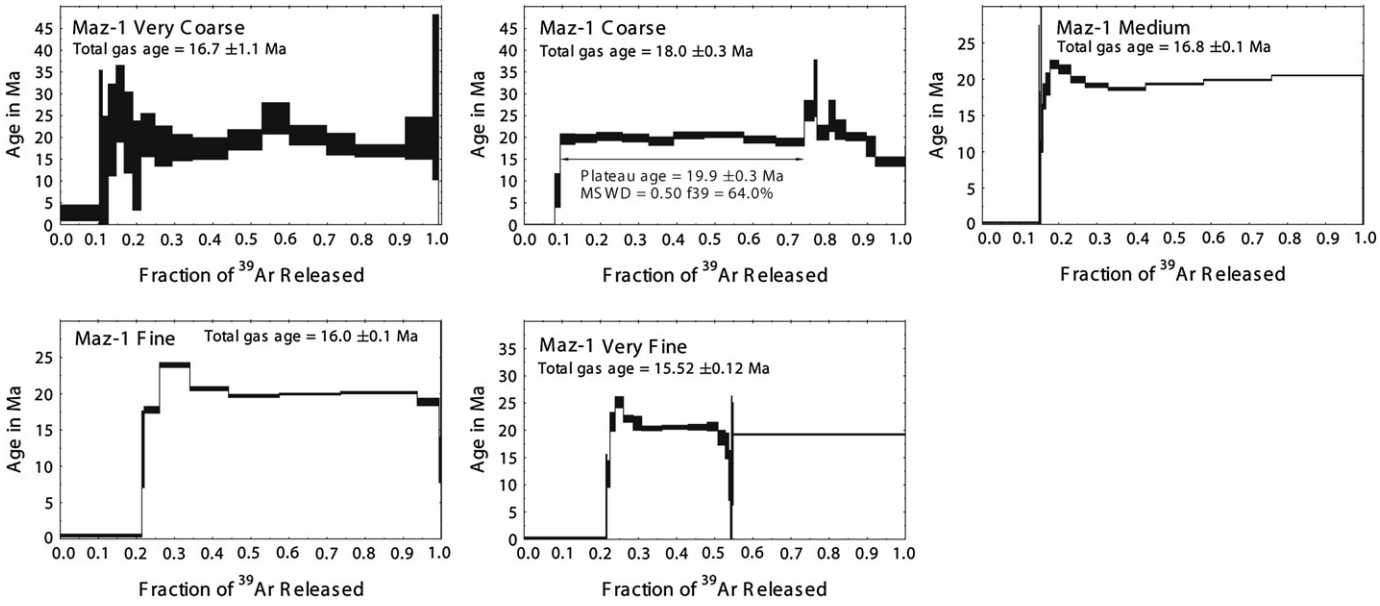

Fig. 11. Ar–Ar spectra for the five size fractions of gouge from Sierra Mazatán.

constant of argon that is linearly proportional to the percentage detrital mica. The illite age analysis plot for the gouge sample from Sierra Mazatán is shown in Fig. 12, and indicates a 14.9 Ma for the age of the authigenic component, and an 18.9 Ma age for the detrital component.

6. Interpretation and discussion

The 14.9 Ma age of the $1M_d$ component of the gouge is the age of authigenic illite growing in the fault gouge. As the gouge sample was crudely foliated and but was not itself brecciated, it can be inferred that the illitic gouge formed under conditions of significant differential stress, and thus during the period the fault was active. The preservation of this syntectonic fabric also indicates that any post-illite-growth slip was extremely minor. Thus it is clear that the age of the authigenic illite is also the age of the last major slip episode on the fault, and that the currently outcropping portion of the fault surface was last active at temperatures between 50 and 150 °C, the growth conditions for 1Md illite (Grathoff et al., 2001). Whether the authigenic illite formed during individual slip events, gradually during aseismic creep, or between individual seismic events due to fluid flow along the fault, remains unclear.

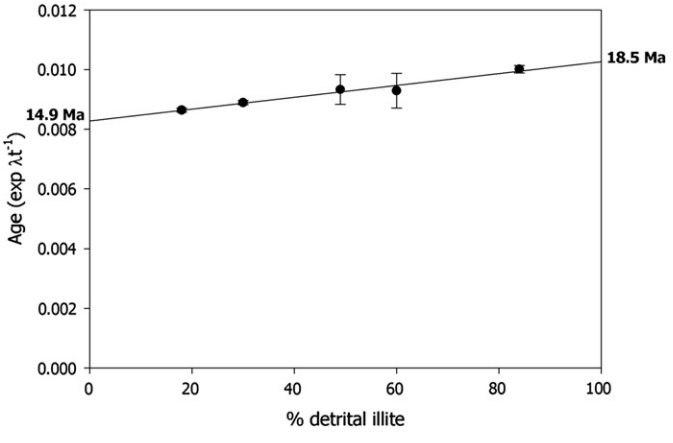

Fig. 12. Illite age analysis plot for gouge from Sierra Mazatán detachment fault. Numbers in bold are the extrapolated ages for the authigenic (14.9 Ma) and detrital illite populations (18.5 Ma) mixed in the gouge. Percentage detrital illite ($2M_1$) is plotted against function $e^{\lambda t} - 1$, where λ is the decay constant of potassium, and t is time; the percentage of detrital illite is linearly related to the decay constant of potassium and not to chronological time.

The 14.9 Ma gouge age (Fig. 12) fits very well with known field constraints on faulting and demonstrates the reliability of the technique. The gouge age is clearly younger than the constraints imposed by the feldspar age and older than the field constraint on the fault surface imposed by the 12.4 Ma ignimbrite (Wong and Gans, 2003). The cooling history of Wong and Gans (2003) from the M1 locality in the immediate vicinity of the footwall records cooling from 350 °C at 18 Ma to 200 °C at 16 Ma. The 18.5 Ma age of the $2M_1$ component of the gouge extrapolated from the illite age analysis agrees well with the constraints from the M1 feldspar age. The history for the M1 locality records rapid cooling of the immediate footwall of the detachment from 350 °C at 18 Ma, a temperature very close to the 375 ± 25°C Ar blocking temperature of muscovite (Fig. 13).

The age of the authigenic illite also has implications for the rate of fault slip. While Wong and Gans (2003) proposed that rapid slip ceased shortly after 16 Ma, our gouge age indicates slip on the detachment into the purely brittle regime to ~14.9 Ma. The $1M_d$ age indicates cessation of the fault at conditions of 50–150 °C. Wong and Gans (2003) determined slip rates in the plastic regime of 3.3–7.7 mm year^{-1}, broadly consistent with those known from other core complexes (Brady, 2002; Carter et al., 2006). Assuming a geothermal gradient of 25 °C

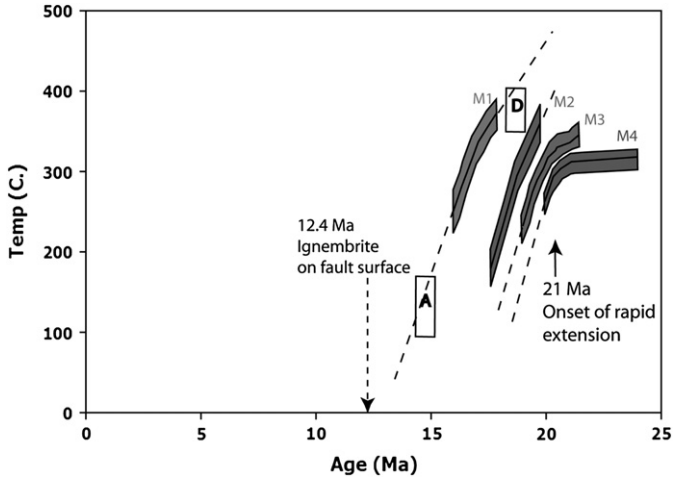

Fig. 13. Summary plot of age data from the Sierra Mazatán detachment. K-feldspar cooling data are from Wong and Gans (2003), "A" is age of authigenic component extrapolated from illite age analysis of gouge (14.9 Ma), "D" is age of detrital component (18.5 Ma).

km^{-1}, an initial fault dip of 60° and growth conditions for $1M_d$ illite to be ~100 °C, the fault accommodated 4 km of slip between 16 Ma and 14.9 Ma, implying a net slip rate of 4.2 ± 2.1 mm $year^{-1}$ and a strain rate on the order of 10^{-14} s^{-1}. It appears that the Sierra Mazatán detachment continued slipping well into the brittle regime at rates similar to those for the plastic regime.

Another consequence of the 18.5 Ma age of the detrital component is that the hanging wall of the detachment contributed little or no detrital material to the gouge. The hanging-wall of the Sierra Mazatán detachment in the vicinity of the gouge outcrop is Cretaceous in age (Vega Granillo and Calums, 2003; Wong and Gans, 2003). Should any appreciable amount of hanging-wall material have contributed to the gouge, the age of the detrital component would have been significantly older than the 18.5 Ma age of the detrital component determined by illite age analysis. This observation of only one wall of a fault zone contributing the vast majority of detrital material in gouge is at variance with the widely described fault structure of a high-strain fault core surrounded by a symmetrical lower-strain damage zone (cf. Chester and Logan, 1987), but is consistent with macroscopic observations in other metamorphic core complexes (Hayman, 2006).

7. Conclusions

Illite polytype quantification using calculated WILDFIRE© patterns accurately quantifies artificial mixtures of $2M_1$ and $1M_d$ illite and supports the application to natural mixtures in real fault gouge. Polytype quantification is significantly improved when the effects of background broadening are considered, particularly with $2M_1$-rich mixtures.

Both the ages of the detrital and authigenic components at Sierra Mazatán extrapolated from illite age analysis of gouge fit remarkably well with regional constraints. The assumption in illite age analysis that gouge is a mixture of two populations of illites, one detrital, derived from the wall rock, and one authigenic forming in the brittle fault zone is therefore supported, as well. The 18.5 Ma age extrapolated for the detrital component ($2M_1$ illite or muscovite) matches well with the time at which the footwall of the detachment passed through the closure temperature of muscovite. The 14.9 Ma age for the age of the latest period of faulting and fluid flow at the Sierra Mazatán metamorphic core complex directly constrains the end of activity on the detachment of this metamorphic core complex. The gouge age indicates that high slip rates from 2.1 mm $year^{-1}$ to 6.9 mm $year^{-1}$ inferred from the plastic regime continued into the brittle regime.

Acknowledgments

This study was funded by NSF grants EAR-0230055 and EAR-0345985, and the Turner Fund of the Department of Geological Sciences at the University of Michigan. In particular, we wish to thank Martin Wong for his help in providing sample material and advice on the geology of Sierra Mazatán. We also thank Chris Hall and Marcus Johnson for assistance with Ar dating, and Carl Henderson for maintenance of the EMAL-XRD facility. Thoughtful reviews by Sarah Sherlock and Laurence Warr helped us to clarify the presentation and arguments of the paper.

References

Anderson, T., Silver, L., Salas, G., 1980. Distribution and U–Pb isotopic ages of some lineated plutons, northwest Mexico. Geological Society of America Memoir 153, 269–283.

Bailey, S., 1988. X-ray diffraction identification of the polytypes of mica, serpentine, and chlorite. Clays and Clay Minerals 36, 193–213.

Bailey, S., Hurley, P., Fairbairn, H., Pinson, W., 1962. K–Ar dating of sedimentary illite polytypes: Geological Society of America Bulletin 73, 1167–1170.

Brady, R., 2002. Very high slip rates on continental extensional faults: New evidence from (U/Th)/He thermochronometry of the Buckskin Mountains, Arizona. Earth and Planetary Sciences Letters 197, 97–104.

Carter, T., Kohn, B., Foster, D., Gleadow, A., Woodhead, J., 2006. Late stage evolution of the Chemehuevi and Sacramento detachment faults from apatite (U/Th)/He thermochronometry – evidence for mid-Miocene accelerated slip. Geological Society of America Bulletin 118, 689–709.

Chester, F., Logan, J., 1987. Composite planar fabric of gouge from the Punchbowl Fault, California. Journal of Structural Geology 9, 621–634.

Clauer, N., Srodon, J., Francu, J., Sucha, V., 1997. K-Ar dating of illite fundamental particles seperated from illite-smectite. Clay Minerals 32, 181–196.

Dalla Torre, M., Stern, W., Frey, M., 1994. Determination of white mica polytype ratios: comparison of different XRD methods. Clay Minerals 29, 717–726.

Dong, H., Hall, C., Peacor, D., Halliday, A., 1995. Mechanism of argon retention in clays revealed by laser ^{40}Ar–^{39}Ar dating. Science 267, 355–359.

Dong, H., Hall, C., Halliday, A., Peacor, D., 1997. ^{40}Ar–^{39}Ar dating of late-Caledonide (Acadian) metamorphism and cooling of K-bentonites and slates from the Welsh Basin. UK. Earth and Planetery Science Letters 150, 337–351.

Drits, V.A., Plançon, A., Sakharov, B.A., Besson, G., Tsipursky, S.I., Tchoubar, C., 1984. Diffraction effects calculated for structural models of K-saturated montmorillonite containing different types of defects. Clay Minerals 19, 541–562.

Gans, P., 1997. Large-magnitude Oligo-Miocene extension in southern Sonora: implications for the tectonic evolution of northwest Mexico. Tectonics 16, 388–403.

Grathoff, G., Moore, D., 1996. Illite polytype quantification using WILDFIRE – calculated patterns. Clays and Clay Minerals 44, 835–842.

Grathoff, G., Moore, D., Hay, R., Wemmer, K., 1998. Illite polytype quantification in Paleozoic shales: a technique to quantify diagenetic and detrital illite. In: Schieber, J., et al. (Eds.), Shale and Mudstones II. Petrography, Petrophysics, Geochemistry, and Economic Geology. Schweizerbartsche Verlagsbuchhandlung, Stuttgart, Germany, pp. 161–175.

Grathoff, G., Moore, D., Hay, R., Wemmer, K., 2001. Origin of illite in the lower Paleozoic of the Illinois Basin: evidence for brine migration. Geological Society of America Bulletin 113, 1092–1104.

Harrison, M., Grovem, M., Lovera, O., Zeitler, P., 2005. Continuous thermal histories from inversion of closure profiles. Reviews in Mineralogy and Geochemistry 58, 389–409.

Hayman, N., 2006. Shallow crustal fault rocks from the Black Mountain detachments, Death Valley, CA. Journal of Structural Geology 28, 1767–1784.

Hower, J., Hurley, P.M., Pinson, W.H., Fairbairn, H.W., 1963. The dependence of K-Ar age on the mineralogy of various particle size ranges in a shale. Geochimica et Cosmochimica Acta 27, 405–410.

Hower, J., Mowatt, T., 1966. The mineralogy of illites and mixed-layer illite/montmorillonites. American Mineralogist 51, 825–854.

Kralik, M., Klima, K., Riedmueller, G., 1987. Dating fault gouges. Nature 327, 315–317.

Levenson, A.A., 1955. Studies in the mica group: polymorphism among illites and hydrous micas. American Mineralogist 40, 41–49.

Lonker, S., Fitz Gerald, J., 1990. Formation of coexisting 1M and 2M polytypes in illite from an active hydrothermal system. American Mineralogist 75, 1282–1290.

Lyons, J., Snellenburg, J., 1970. Dating faults. Geological Society of America Bulletin 82, 1749–1752.

McDougall, I., Harrison, M., 1999. Geochronology and Thermochronology by the $^{40}Ar/^{39}Ar$ Method. Oxford Monographs on Geology and Geophysics No. 9, second ed. Oxford University Press, New York, 212 pp.

McGrew, A., Snee, L., 1994. $^{40}Ar/^{39}Ar$ thermochronologic constraints on the tectonothermal evolution of the northern East Humboldt Range metamorphic core complex, Nevada. Tectonophysics 238, 425–450.

Miller, E., Dumitru, T., Brown, R., Gans, P., 1999. Rapid Miocene slip on the Snake Range–Deep Creek fault system, east-central Nevada. Geological Society of America Bulletin 111, 886–905.

Miller, J., John, B., 1999. Sedimentation patterns support seismogenic low-angle normal faulting, southeastern California and western Arizona. Geological Society of America Bulletin 111, 1350–1370.

Moore, D.M., Reynolds Jr., R.C., 1997. X-ray Diffraction and the Identification and Analysis of Clay Minerals. Oxford University Press, New York.

Nourse, J., Anderson, T., Silver, L., 1994. Tertiary metamorphic core complexes in Sonora, northwest Mexico. Tectonics 13, 1161–1182.

Peacor, D.R., Bauluz, B., Dong, H., Tillick, D., Yan, Y., 2002. TEM and AEM evidence for high Mg contents of 1M illite. Absence of 1M polytypism in normal prograde diagenetic sequences. Clays and Clay Minerals 50, 757–765.

Pevear, D.R., 1992. Illite age analysis, a new tool for basin thermal history analysis. In: Kharaka, Y.K., Maest, A.S. (Eds.), Proceedings of the 7th International Symposium on Water-Rock Interaction. Balkema, Rotterdam, Netherlands, pp. 1251–1254.

Pevear, D.R., 1999. Illite and hydrocarbon exploration. Proceedings of the National Academy of Sciences 96, 3440–3446.

Reynolds, R., 1963. Potassium-rubidium ratios and polymorphism in illites and microclines from the clay size fractions of proterozoic carbonate rocks. Geochimica et Cosmochimica Acta 27, 1097–1112.

Reynolds, Jr., R., 1993. WILDFIRE – A Computer Program for the Calculation of Three-dimensional Powder X-ray Diffraction Patterns for Mica Polytypes and their Disordered Variations. Hanover, NH.

Reynolds, Jr., R., Reynolds, III, R., 1996. NEWMOD-for-Windows. The Calculation of One-Dimensional X-ray Diffraction Patterns of Mixed-layered Clay Minerals. Hanover, NH, 1996.

Shimoda, S., 1970. A hydromuscovite from the Shakani mine, Akita Prefacture, Japan. Clays and Clay Minerals 18, 267–274.

Smith, J., Yoder, H., 1956. Experimental and theoretical studies of the mica polymorphs. Mineralogical Magazine 31, 209–231.

Solum, J., van der Pluijm, B., 2005. Neocrystallization, fabrics and age of clay minerals from an exposure of the Moab fault zone, Utah. Journal of Structural Geology 27, 1563–1576.

Solum, J., van der Pluijm, B., 2007. Reconstructing the Snake River/Hoback Canyon segment of the Wyoming thrust Belt through direct dating of fault rocks. In Whence the Mountains? Inquiries into the Evolution of Orogenic Systems: A volume in Honor of Ray Price. Geological Society of America Memoir 433.

Sroden, J., 1980. Precise identification of illite/smectite interstratifications by X ray powder diffraction. Clays and Clay Minerals 28, 401–411.

Srodon, J., Eberl, D., 1984. In: Bailey, S. (Ed.), Micas, Mineralogical Society of America Reviews in Mineralogy. Illite, 13.

Srodon, J., Elsass, F., McHardy, W., Morgan, D., 1992. Chemistry of illite-smectite inferred from TEM measurements of fundamental particles. Clay Minerals 27, 137–158.

van der Pluijm, B., Hall, C., Vrolijk, P., Pevear, D., Covey, M., 2001. The dating of shallow faults in the Earth's crust. Nature 412, 172–175.

van-der-Pluijm, B., Vrolijk, P., Pevear, D., Hall, C., Solum, J., 2006. Fault dating in the Canadian Rocky Mountains: Evidence for late Cretaceous and early Eocene orogenic pulses. Geology 34, 837–840.

Vanderhaeghe, O., Teyssier, C., McDougall, I., Dunlap, W.J., 2003. Cooling and exhumation of the Shuswap Metamorphic Core Complex constrained by $^{40}Ar/^{39}Ar$ thermochronology. Geological Society of America Bulletin 115, 200–216.

Vega Granillo, R., Calmus, T., 2003. Mazatan metamorphic core complex (Sonora, Mexico): structures along the detachment fault and its exhumation evolution. Journal of South. American Earth Sciences 16, 193–204.

Velde, B., Hower, J., 1963. Petrological significance of illite polymorphism in Paleozoic sedimentary rocks. American Mineralogist 48, 1239–1254.

Velde, B., 1965. Experimental determination of muscovite polymorph stabilities. American Mineralogist 50, 436–449.

Vrolijk, P., van der Pluijm, B., 1999. Clay gouge. Journal of Structural Geology 21, 1039–1048.

Weaver, C., Brockstra, B., 1984. Illite-mica. In: Weaver, C., et al. (Eds.), Shale Slate Metamorphism in the Southern Appalachian Mountains. Elsevier, Amsterdam, pp. 67–199.

Wong, M., Gans, P., 2003. Tectonic implications of early Miocene extensional unroofing of the Sierra Mazatán metamorphic core complex, Sonora, Mexico. Geology 31, 953–956.

Wong, M., Gans, P., 2005. Constraining the slip history and initial dip of low-angle normal faults using $^{40}Ar/^{39}Ar$ K-feldspar thermochronology: a case study from the Sierra Mazatán core complex, Sonora, Mexico. Abstracts, Goldschmidt Conference A293.

Yan, Y., van der Pluijm, B., Peacor, D., 2001. Deformational microfabrics of clay gouge, Lewis Thrust, Canada: a case for fault weakening from clay transformation. In: Special Publication, vol. 186. Geological Society, London, pp. 103–112.

Ylagan, R., Kim, C., Pevear, D., Vrolijk, P., 2002. Illite polytype quantification for accurate K-Ar determination. American Mineralogist 87, 1536–1545.

Yoder, H., Eugster, H., 1955. Synthetic and natural muscovites. Geochimica et Cosmochimica Acta 8, 225–280.